

Hot Corrosion Behavior of Plasma Sprayed Coatings on Nickel Based Superalloy in Aggressive Environments at 900°C

Kunal Prasad, Soumava Mukherjee, Kurian Antony, Devendranath Ramkumar K, Arivazhagan N*

School of Mechanical and Building Sciences, VIT University, Vellore 632 014, India

*Corresponding Author: narivazhagan@vit.ac.in

Phone: 91-9443034794

Fax: 91-416-2243092

Abstract

An attempt has been made to study the effects of hot corrosion studies on Inconel-625 substrates with Nickel Chromium, Aluminum Oxide, and Tungsten Carbide coatings using plasma arc spray technique. Hot corrosion studies were conducted on an uncoated Inconel-625 as well as coated samples in molten salt environment ($\text{Na}_2\text{SO}_4 - 60\%\text{V}_2\text{O}_5$) at 900°C to simulate aggressive conditions encountered in industrial applications. The samples were also subjected to air oxidation through a series of repetitive heating and cooling stages. The corrosion rates were determined from the experiments and compared to judge the suitability of the coatings. Techniques like X-Ray Diffraction (XRD), Scanning Electron Microscopy (SEM) and Energy Dispersive X-ray Analysis (EDAX) were used to characterize the corrosion products.

Keywords: Plasma Spray, Super Alloy, Hot Corrosion.

1. Introduction

Materials are often exposed to hot corrosive environments in industrial applications and are subject to degradation over time ultimately resulting in failure. Since aggressive environments are very common in industries, it is necessary to use materials that can sustain high temperatures and perform satisfactorily while providing a better service life. Hot corrosion is a high-temperature analog of aqueous atmospheric corrosion. A thin film deposit of fused salt on an alloy surface in a hot oxidizing gas causes accelerated corrosion kinetics.

A superalloy is an alloy that exhibits excellent mechanical strength and resistance to creep at high temperatures, good surface stability and corrosion and oxidation resistance. Superalloy development has relied heavily on both chemical and process innovations and has been driven primarily by the aerospace and power industries. Inconel-625 is a Ni-Cr-Mo alloy and a trademark of special metals Corporation. Inconel-625 is used for its high strength, excellent fabricability (including joining) and outstanding corrosion resistance. Service temperatures range from cryogenic to 1800°F (982°C). Coatings provide a way of extending the limits of use of materials at the upper end of their performance capabilities.

A combination of Ni-Cr coating is corrosion-resistant and has a high melting point of about 1400°C. Ni-Cr wire is used because of its ability to withstand the high temperatures that occur when clay work is fired in a kiln. In the experiment Ni-Cr alloy powder was sprayed on boiler steels by the cold spray process, which resulted in a dense adherent and oxide free coatings on the steels. Ni-Cr cold spray coatings were found to have significantly higher Micro-hardness in comparison with SA 516 steels [1]. The cold sprayed Ni-Cr coating on two different substrates when subjected to hot corrosion in $\text{Na}_2\text{SO}_4 + \text{V}_2\text{O}_5$ environment at 900°C was found to be successful in maintaining its adherence with the substrate steels. The oxide scales were also found

to be intact and there was no indication of spalling in both the cases [2–4]. Sidhu et al.[5], found high velocity oxy–fuel coating spraying (HVOF) sprayed NiCrBSi coatings to be effective in imparting hot corrosion resistance to Supernickel–75 in a coal fired boiler environment. The formation of oxides of chromium and cobalt, and spinels of cobalt–chromium (CoCr_2O_4) and nickel–chromium (NiCr_2O_4) for the alloy might be responsible for best performance of this coating.

Whereas alumina coating is serves as for a broad range of advanced ceramic products and as an active agent in chemical processing. Al_2O_3 is an electrical insulator but has a relatively high thermal conductivity for a ceramic material. Metallic aluminum is very reactive with atmospheric oxygen and a thin passivation layer of aluminum oxide (4 nm thickness) forms on any exposed aluminum surface. Harpreet Singh et al. [6] investigated the hot corrosion behavior of HVOF–sprayed NiCrBSi coatings on Ni and Fe–based Superalloys in Na_2SO_4 –60% V_2O_5 environment at 900°C. In this experiment Iron is found to have a relatively higher concentration near the coating–substrate interface which indicates its diffusion behavior from the substrate to the coating. The presence of vanadium and sulfur below the top scale indicates that they have penetrated along the boundaries. The authors [7–9] also reported that the higher spalling of the bare superalloy could be because of severe strain developed by precipitation of Fe_2O_3 from the liquid phase during cooling period of thermal cycles and inter–diffusion of intermediate layers of iron oxide. The cracks might have allowed the aggressive liquid phase to reach the metal substrate. Gurrappa et al. [9], have tested a variety of MCrAlY–type coatings with different alloying elements in the presence of sodium chloride and vanadium containing environments. Results revealed that NiCoCrAlY coating exhibited maximum life time among the coatings studied. The

results also revealed that presence of trace elements in the coating reduced coating life significantly.

Tungsten carbide coating is containing equal parts of tungsten and carbon atoms. At high temperatures WC decomposes to tungsten and carbon and this can occur during high-temperature thermal spray as in high velocity oxygen fuel (HVOF) and high energy plasma (HEP) methods. Oxidation of WC starts at 500–600°C. It is resistant to acids and is only attacked by hydrofluoric acid/nitric acid mixtures above room temperature. According to the Harpreet Singh et al. [6] plasma spray technique can be used to develop coatings of NiCrAlY, Ni-20Cr, etc., on a ferrous based alloy. NiCrAlY coating provided the best protection to the base alloy. Mahesh et al.[1, 4], reported that the rapid increase in the mass gain during the initial period of exposure to molten salt environment at 900°C may be due to the rapid diffusion of oxygen through the molten salt layer. Arivazhagan et al. [10–12] found that corrosion involving a Na₂SO₄–V₂O₅ combination resulted in formation of NaV₆O₁₅ and NaV₃O₈ deposits. The molten salt was very corrosive and increased the acidic solubility of the protective oxides.

Little work has been published on hot corrosion studies on plasma arc spray coated Inconel–625 substrates with Nickel Chromium, Aluminum Oxide, and Tungsten Carbide powders. The objective of the present research work is, therefore, to characterize the plasma arc spray coated Inconel–625 in air and molten salt environments. The superalloys selected for this study have been procured commercially to find suitable protective coatings for extending life of the Inconel 625 at the upper end of their performance capabilities. This alloy have applications in steam boilers, furnace equipment, heat exchangers and piping in the chemical industry, reformers and baffle plates/tubes in fertilizer plants. The hot corroded samples have been characterized using the combined techniques of optical X-ray

diffraction (XRD) and Scanning Electron Microscopy/Energy-Dispersive Analysis (SEM/EDAX).

2. Experiments

The Inconel 625 superalloys used as substrate materials in this study and the nominal chemical composition of the substrate materials is reported in Table 1. The specimens, each measuring approximately 15×15×5 mm, were cut from the alloy sheets, polished with SiC papers down to 180 grit and subsequently grit blasted with alumina powders (Grit 45) before development of the coatings by plasma arc spraying process. Commercially available Ni-Cr, Al₂O₃ and WC powders was used in this study. Standard spray parameters were used for depositing the Stellite-6 coatings. All the process parameters, including the spray distance, were kept constant throughout coating process. The specimens were cooled with compressed air jets during and after spraying. The employed spraying parameters are given in Table 2. The coating thickness has been estimated to be around 70µm and the photographs of coated and un-coated samples are given in Fig 1.

Thermo-gravimetric study was performed in a molten salt (Na₂SO₄ – 60%V₂O₅) environment consisting of 25 cycles on all the samples. A layer of Na₂SO₄-60%V₂O₅ with a uniform thickness of about 3–5 mg/cm² was applied on the surface of the samples after preheating to 200°C for 1 hour. Preheating was done to ensure removal of any moisture. Silica based boats and crucibles were used to contain the samples. Heating was done in a tubular type furnace at a temperature of 900°C. Each cycle comprised of a 2 hour heating period followed by 25 minutes of cooling in air at room temperature.

The weights of the different specimens were recorded after physical observation at the end of each cycle with help of an electronic balance had sensitivity of 0.1 mg. Scales and deposits, if any, were also included in weight determination. The kinetics of corrosion was then calculated from the weight measurements. This process was repeated with another set of samples but instead of a molten salt environment the samples were directly subjected to air oxidation. After completion of the thermogravimetric studies, the samples were analyzed using XRD, SEM and EDAX techniques.

3. Results

3.1. Physical Observation

3.1.1. Molten Salt Environment

In case of the uncoated Inconel-625 sample, mild spalling was observed after the completion of the 2nd cycle. Brownish grey scales appeared on the surface possibly due to deposition of as hand turned darker in color over time. The amount of sputtering increased progressively and it was observed that the surface was becoming coarser with the progress of study. About 0.12g of deposits were obtained by the end of the corrosion study. The Ni-Cr coated Inconel 625 sample appeared slightly darker in color after completion of the 1st cycle. Greenish yellow scales were observed on the surface of the boat by the time the 2nd cycle was completed. There was a minor increase in the quantity of scales during the course of experiment. However, no spalling or sputtering was observed until the end of the corrosion study. The coating on the specimen was intact and adherent and didn't show any tendency of crack formation. The WC coated Inconel 625 exhibited minor spalling after completion of the 1st cycle. By the time the 3rd cycle was completed, the surface was found to have bulged a little while the coating was found to be disintegrated by the end of the 6th cycle. In case of the Aluminum

Oxide coated sample, sputtering was observed during the 2nd cycle and the coating was found to be disintegrated by the end of the 6th cycle.

3.1.2. Air Oxidation Mode

In case of the uncoated Inconel–625 sample spalling and sputtering was observed after completion of the 4th cycle. Greyish scales appeared on the surface of the boat and the scales turned dark in color with the course of the study. In case of the Ni–Cr coated Inconel–625 sample no spalling or sputtering was observed. However, greenish yellow scales appeared on the surface of the boat after the completion of 4th cycle. The Aluminum oxide and Tungsten Carbide coatings, however were not sustained beyond 7 cycles and were found to be disintegrated

3.2 Corrosion Kinetics

The coated samples as well as the samples after hot corrosion studies are represented in Fig 1–2. Graphs of weight change per unit area versus number of cycles are plotted for the bare and coated samples undergoing corrosion in molten salt and air oxidation modes. The weight change consists of a weight gain owing to the formation of the oxide scales and a weight loss due to the suspected spalling and fluxing of the oxide scales. The net weight change of the specimens in the given environment represents the combined effects of these two processes. The coated specimen i.e. Ni–Cr coated Inconel 625 has shown less weight gain than the uncoated bare substrate. (Weight change/area)² vs. number of cycles plot for coated and uncoated samples are shown in Fig 3–7 to establish the parabolic rate law of hot corrosion. The plot for the bare Superalloy shows observable deviations from the parabolic path, while the fluctuations in data are quite less for coated specimen. Overall, the coated sample was found to have followed nearly parabolic behavior up to 23 cycles.

The parabolic rate constant k_p is calculated by a linear least-square algorithm to a function in the form of $(\Delta W/A)^2 = k_p \times t$, where $\Delta W/A$ is the weight gain per unit surface area (mg/cm^2) and t is the hot corrosion time in seconds. The parabolic rate constants (k_p) for the uncoated and Ni-Cr coated Inconel-625 samples are shown in Table 3.

3.3 X-Ray Diffraction Analysis

The XRD analysis was carried out on a Bruker AXS D-8Advance Diffractometer with $\text{Cu-K}\alpha$ radiation. The XRD patterns of the samples are shown in Fig 8-15. XRD patterns of hot corroded Ni-Cr coated sample revealed presence of NiO, NiCr_2O_4 and Cr_2O_3 . Several weak phases of Ni_3C were also identified. Bare alloy Inconel-625 was found to have Fe_2O_3 , Cr_2O_3 , FeVO_4 , FeV_2O_4 , NiCr_2O_4 and NiO as the major phases. Traces of WO_2 and WO_3 was found in the WC coated sample besides the oxides of Nickel and Chromium while NiAl_2O_4 and other oxides of Nickel and Chromium were found to have been formed in the Aluminum Oxide coated sample. The various phases identified with the XRD Analysis for both bare and coated samples are presented in Table 4.

3.4 SEM/EDAX Analysis

SEM micrographs with EDAX analysis at selected points revealed nature of the samples after corrosion study. In case of bare Inconel-625 alloy, large numbers of small pores were seen on the surface of the specimen. The major oxides formed on the surface were those of Cr_2O_3 and NiCr_2O_4 along with a small percentage of NiO. The scales formed on the uncoated Inconel 625 sample had a rough surface with embedded ash

grains. Black spots observed on the scale were the regions from where suspected spallation of the scales might have occurred and these regions were found to be rich in Fe_2O_3 along with ash deposits and little amounts of FeVO_4 , FeV_2O_4 and Cr_2O_3 . Presence of Fe_2O_3 , FeVO_4 and FeV_2O_4 in the surface indicated their outward diffusion from the substrate through the coatings. Continuous, uniform and adherent oxide scales rich in NiO , NiCr_2O_4 and Cr_2O_3 were found on the Ni-Cr coated Inconel-625 sample without any indication of crack formation. SEM Micrographs along with EDAX of the different samples are shown in Fig 16–19.

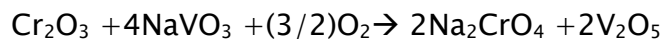
4. Discussion

It was observed that all specimens (coated and uncoated) were prone to weight gain upon exposure to high temperatures (Fig 3–7). Although weight gain was high initially, it got leveled over time and change in weight was comparatively less in the later stages. The rapid increase in mass during initial periods of exposure may be due to rapid diffusion of oxygen through the molten salt layers. Coatings are generally sacrificial in nature and act as a reservoir for the formation of oxides or spinels and are prone to rapid oxidation during the initial stages. It has been proposed by Arivazhagan et al.[13] that in the temperature range of 900°C , the Na_2SO_4 and V_2O_5 will combine to form NaVO_3 , as represented below, while having a melting point of 610°C .



This NaVO_3 acts as a catalyst and also serves as an oxygen carrier to the base alloy. Through the open pores present on the surface, NaVO_3 will lead to the rapid oxidation of the base elements to form a protective oxide scale. There may also be simultaneous

dissolution of Cr_2O_3 in the molten salt due to the reaction as per the equation shown below.



During the subsequent cycles, formation of oxides may block the diffusion of corrosive species by covering the pores. In case of the uncoated alloy, Iron was found to have diffused from the surface and was subsequently oxidized to Fe_2O_3 . Compounds like FeVO_4 and FeV_2O_4 were also formed. From SEM/EDAX analysis presences of small pores were seen on the surface of the bare alloy (after corrosion study) thereby indicating possible escape of vaporized phases (Fig 16–19). These pores can help corroding species to easily penetrate into the substrate and cause damage. Intensive spalling/sputtering of the uncoated alloy can be attributed to severe strain developed due to the precipitation of Fe_2O_3 from the liquid phase and inter-diffusion of intermediate layers of iron. Further, the presence of different phases in a thin layer might have imposed severe strain on the film, which resulted in cracking and peeling of the scale. The cracks may have allowed the aggressive liquid phase to reach the metal substrate. Titanium, Iron and cobalt have a high affinity towards oxygen, so it showed a tendency to diffuse outward from the substrate through the coating and formed an oxide layer at the top most part of the scale. However after initial hours of exposure, oxides of chromium and silicon that might have possibly formed at the splat boundaries could have acted as diffusion barriers and restricted allowance of other species in the scale–substrate interface. In case of the Ni–Cr coated Inconel–625 it was observed that the greenish–yellow oxide scales were intact with the coating and spalling was almost negligible. The greenish color of the scale may be due to the presence of NiO . Weight gain per unit area observed in uncoated Inconel–625 sample was found to be less than that of Ni–Cr coated Inconel–625 sample. However, Ni–Cr

coating was found to give protection against spalling and sputtering in aggressive environment of $\text{Na}_2\text{SO}_4 - 60\%\text{V}_2\text{O}_5$ at 900°C . The XRD analysis of the Ni-Cr-coated sample indicated formation of NiO, Cr_2O_3 , NiCr_2O_4 and spinels of nickel and chromium (Fig 8–15). Very low porosity and the flat splat structure of the Plasma Arc coatings usually contribute towards developing hot corrosion resistance of coated specimens. Due to dense and flat structure of the coatings, the distance from the coating surface to coating/substrate interface is generally very long. This helps in providing protection against hot corrosion. The WC and Al_2O_3 coatings have shown least resistance among the coatings studied which may be attributed to extensive spalling of the oxide scales and the coating itself. Maximum cracking/spalling was observed in WC coated sample whereas it was least (almost negligible) in case of Ni-Cr coating. Spalling of WC and Al_2O_3 coatings may be ascribed to different values of thermal expansion coefficients of the coatings and the substrate. Further, the corrosive environment could have quickly reached the base metal through cracks, resulting in adhesion loss and subsequent spalling of the coating.

5. Conclusion

In the present work, hot corrosion behavior of Plasma sprayed coatings on Inconel–625 in aggressive environment of $\text{Na}_2\text{SO}_4 - 60\%\text{V}_2\text{O}_5$ at 900°C has been investigated and the following conclusions are made:–

- a) The Plasma Arc spray process can be used successfully to deposit Ni-Cr coatings on Inconel–625.
- b) Aluminum Oxide and Tungsten Carbide coatings have refused to adhere to Inconel–625 substrate on exposure to high temperatures possibly due to large variances in coefficient of thermal expansions.

- c) The uncoated superalloy has shown intensive spalling and sputtering during hot corrosion studies in aggressive environment of Na_2SO_4 – 60% V_2O_5 at 900°C.
- d) There is perceptible diffusion of elements like iron and cobalt from the uncoated Inconel–625 substrate to the surface as confirmed by XRD and EDAX techniques.
- e) Ni–Cr coating was found to give protection against spalling and sputtering in aggressive environment of Na_2SO_4 – 60% V_2O_5 at 900°C. This could be due to the formation of NiCr_2O_4 , which might have blocked the diffusion of corrosive species into the substrate.
- f) The oxides of chromium and nickel might have contributed for blocking the transport of degrading species and provided hot corrosion resistance

References

- [1] ‘A study on hot corrosion behaviour of Ni–5Al coatings on Ni–andFe–based superalloys in an aggressive environment at 900°C’, R.A. Mahesh, R. Jayaganthan, S. Prakash, *Journal of Alloys and Compounds*, **460**,1,pp 220–231, 2008.
- [2] ‘Hot corrosion behaviour of HVOF–sprayed NiCrBSi coatings on NiandFe–based superalloys in Na_2SO_4 –60% V_2O_5 environment at 900°C’, T.S. Sidhu, S. Prakash, R.D. Agrawal, *Acta Materialia*, **54**, pp773–784, 2006.
- [3] ‘Hot corrosion studies of HVOF NiCrBSi and Stellite–6 coatings on aNi–based superalloy in an actual industrial environment of a coal fired boiler’, T.S. Sidhu, S. Prakash, R.D. Agrawal, *Surface & Coatings Technology*, **201**, pp1602–1612, 2006.

- [4] 'A study on hot corrosion behaviour of Ni-5Al coatings on Ni- and Fe-based superalloys in an aggressive environment at 900°C', R.A. Mahesh, R. Jayaganthan, S. Prakash, *Journal of Alloys and Compounds* **460** pp220-231, 2007.
- [5] 'Hot corrosion studies of HVOF sprayed Cr₃C₂-NiCr and Ni-20Cr coating on nickel-based superalloy at 900°C', T.S. Sidhu, S. Prakash, R.D. Agrawal, *Surface & Coatings Technology*, **201** pp792-800, 2006.
- [6] 'Some studies on hot corrosion performance of plasma sprayed coatings on a Fe-based superalloy', Harpreet Singh, D. Puri, S. Prakash, *Surface & Coatings Technology*, **192**, pp27- 38, 2005.
- [7] 'Y₂O₃-sealed Ni-Al protective coatings for Inconel 625', T. Sugama, *Surface and Coatings Technology*, **106**, pp106-116, 1998.
- [8] 'Hot corrosion of some superalloys and role of high-velocity oxy-fuel spray coatings', T.S Sidhu, R.D. Agrawal, S. Prakash, *Surface & Coatings Technology*, **198**, pp441- 446, 2005.
- [9] 'Identification of hot corrosion resistant MCrAlY based bondcoatings for gas turbine engine applications', Gurrappa, *Surface and Coatings Technology*, **13**, pp272-283, 2001.
- [10] 'Investigation on AISI 304 Austenitic Stainless Steel to AISI 4140 Low Alloy Steel Dissimilar Joints by Gas Tungsten Arc, Electron Beam and Friction Welding', Arivazhagan N, Surendra Singh, Satya Prakash, G. M. Reddy, *Materials and Design*, **32** , pp3036-3050, 2011.

- [11] 'High temperature corrosion studies on friction welded low alloy steel and stainless steel in air and molten salt environment at 650°', Arivazhagan N, Narayanan S, Surendra Singh, Satya Prakash, G.M.Reddy, *Materials and Design* **34** , pp459–468, 2012.
- [12] 'The influence of welding parameters and temperature of exposure on hot corrosion behavior of friction welded AISI 4140 and AISI 304 in K₂SO₄ – 60%NaCl mixture', Arivazhagan N, Senthilkumaran K, Narayanan S, Devendranath Ramkumar K, Surendra S, Prakash S, *Journal of Materials Science & Technology* , **28**,10, pp895–904, 2012.

Table 1. Chemical composition of Inconel-625

Element	Ni	Cr	F	M	Nb+T	C	Mn	Si	P	S	Al	Ti	Co
Wt%	58	2	5	10	4.15	0.1	0.5	0.5	0.0	0.0	0.4	0.4	1.0
						0	0	0	2	2	0	0	0

Table 2. The process parameters of the plasma arc spraying system

Parameter	Value
Flow Rate / Argon Gas (lpm)	90
Flow Rate / Hydrogen Gas(lpm)	18
Current(Ampere)	500
Voltage(Volts)	65
Powder Feed(grams/min)	45
Spray Distance(inches)	3

Table 3. Calculated valued of Parabolic Rate constant $K_p(10^{-10} \text{ g}^2 \text{ cm}^{-4} \text{ s}^{-1})$

Sample Remarks	Corrosion Mode	
	Molten Salt	Air Oxidation
Ni-Cr coated Inconel-625	0.04	0.105
Un-coated Inconel-625	3.949	3.224

Table 4. Major and Minor Phases detected by XRD Analysis after corrosion study

Description	Major phases	Minor phases
Uncoated Inconel-625	Cr_2O_3 , NiCr_2O_4 , NiO	Fe_2O_3 , FeVO_4 , FeV_2O_4
Ni-Cr coated Inconel-625	NiO , NiCr_2O_4 and Cr_2O_3	Ni_3C
WC coated Inconel-625	WO_3 , WO_2	Cr_2O_3 , NiCr_2O_4 , NiO , CoCr_2O_4
Al_2O_3 coated Inconel-625	NiAl_2O_4 , Al_2O_3	Cr_2O_3 , NiO , NiCr_2O_4 ,

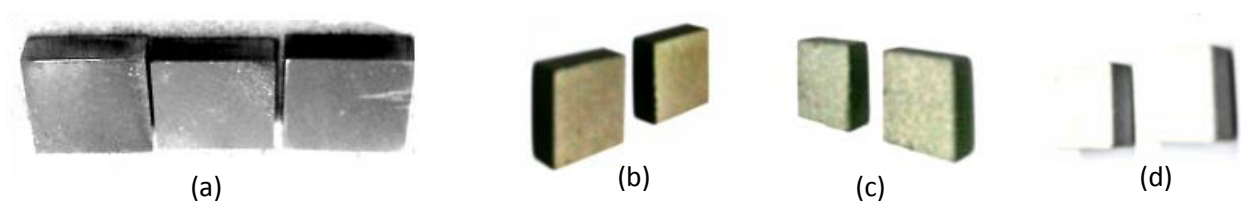


Figure.1

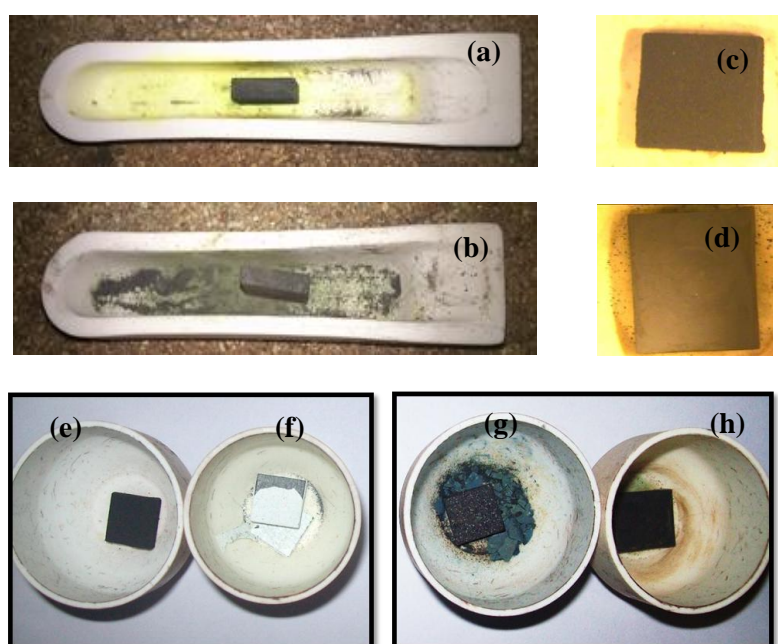


Figure.2

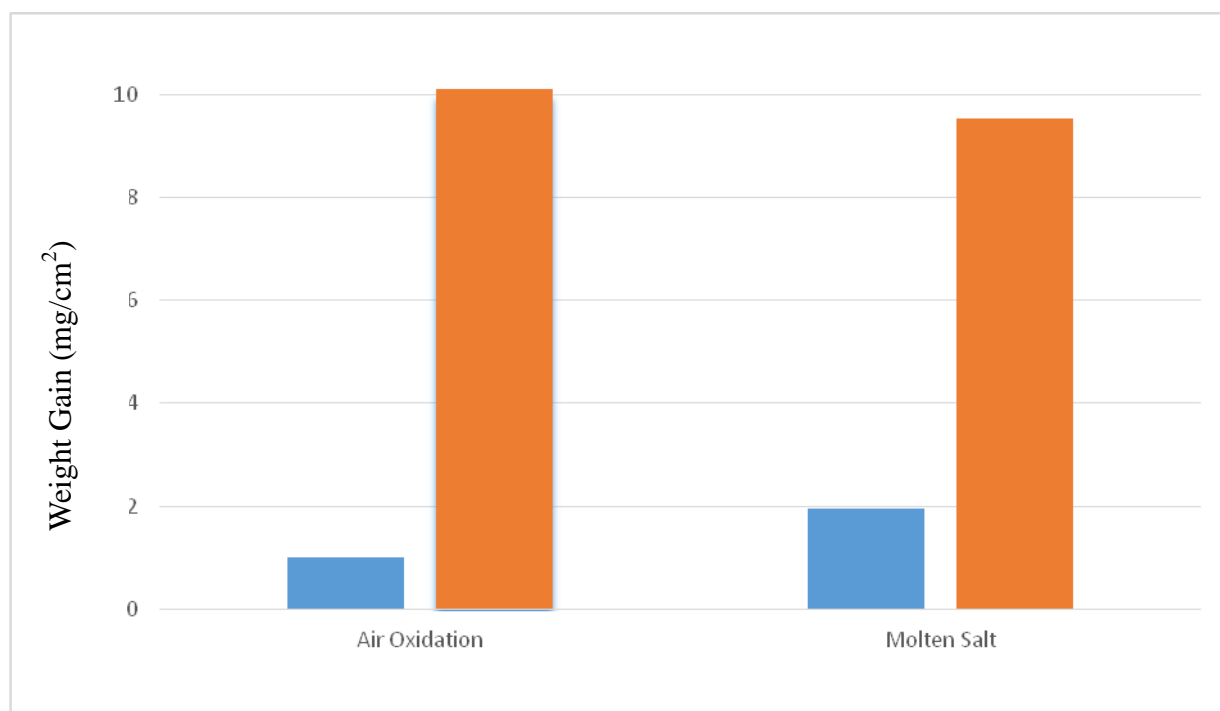


Figure.3

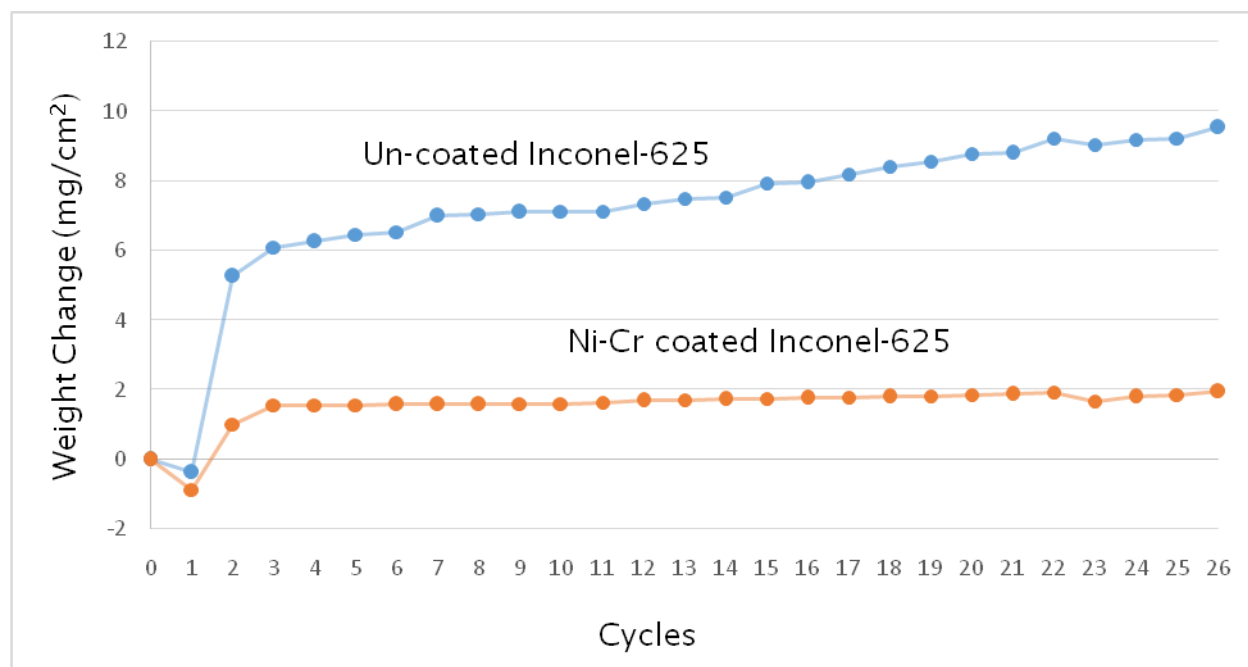


Figure.4

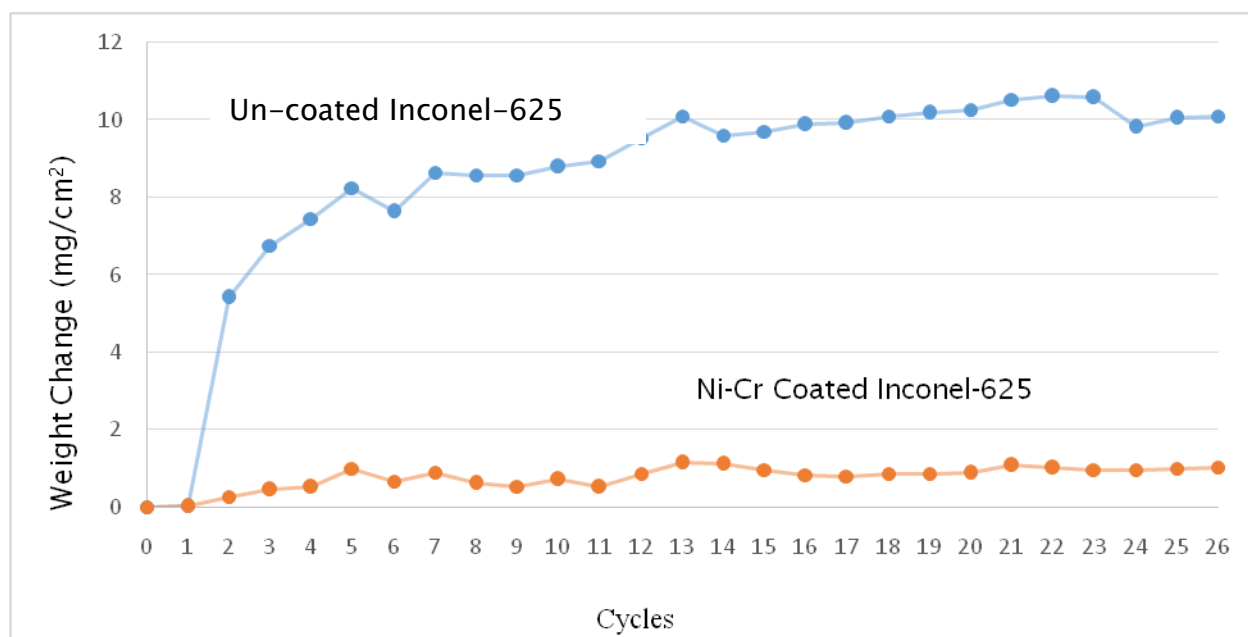


Figure.5

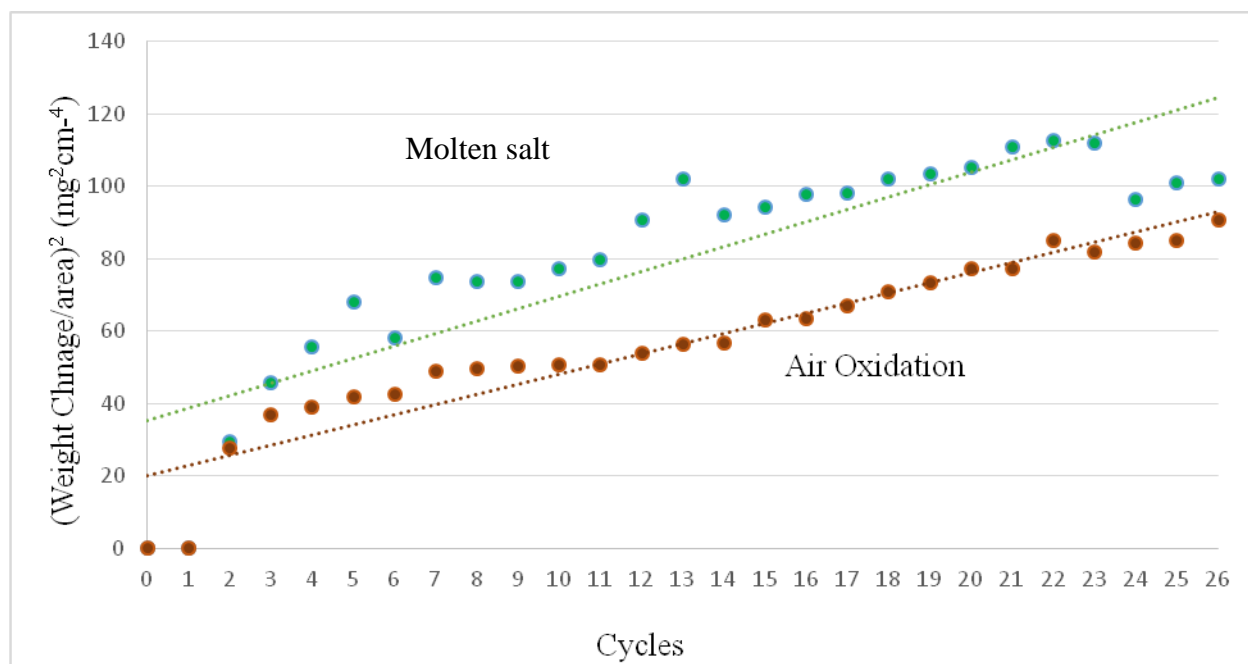


Figure.6

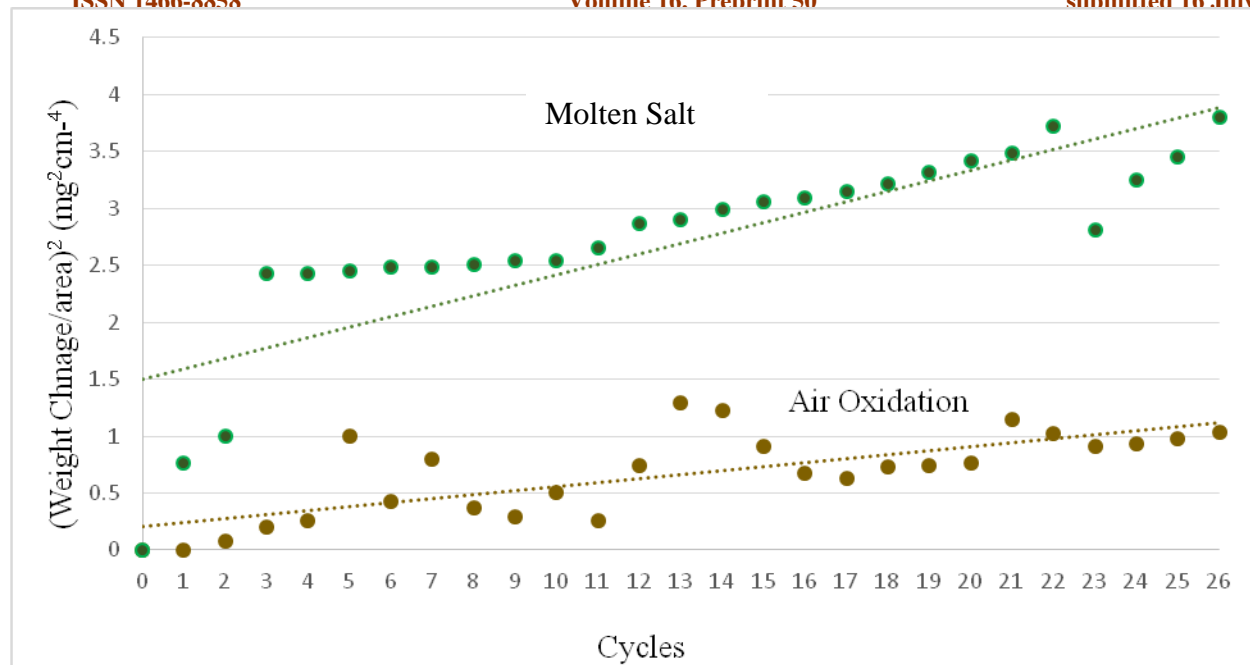


Figure.7

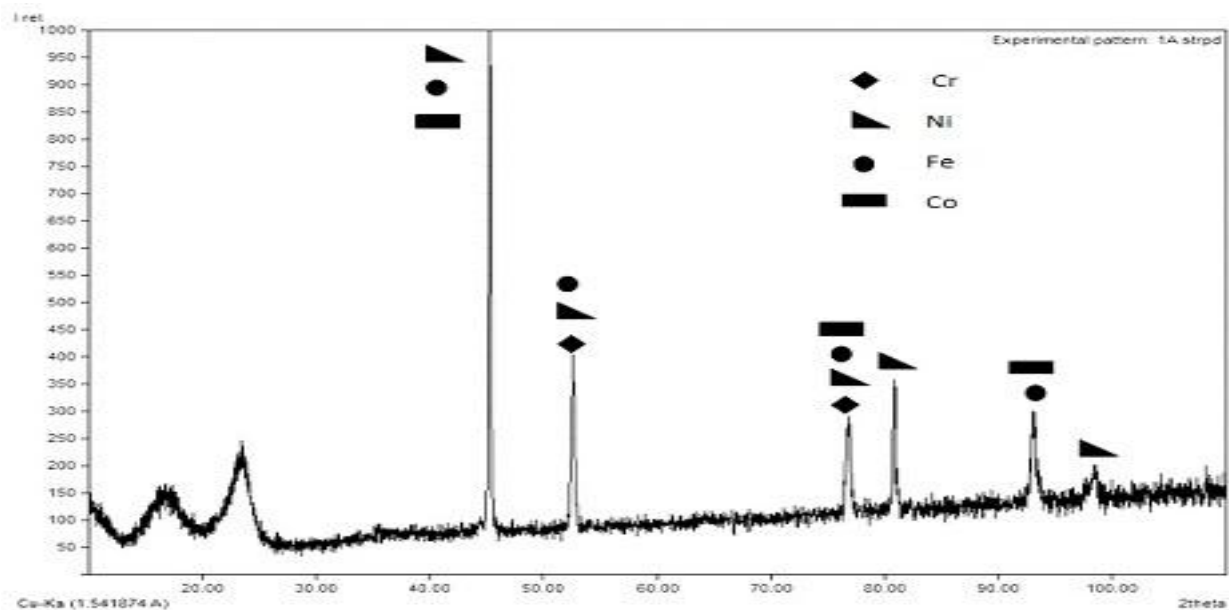


Figure.8

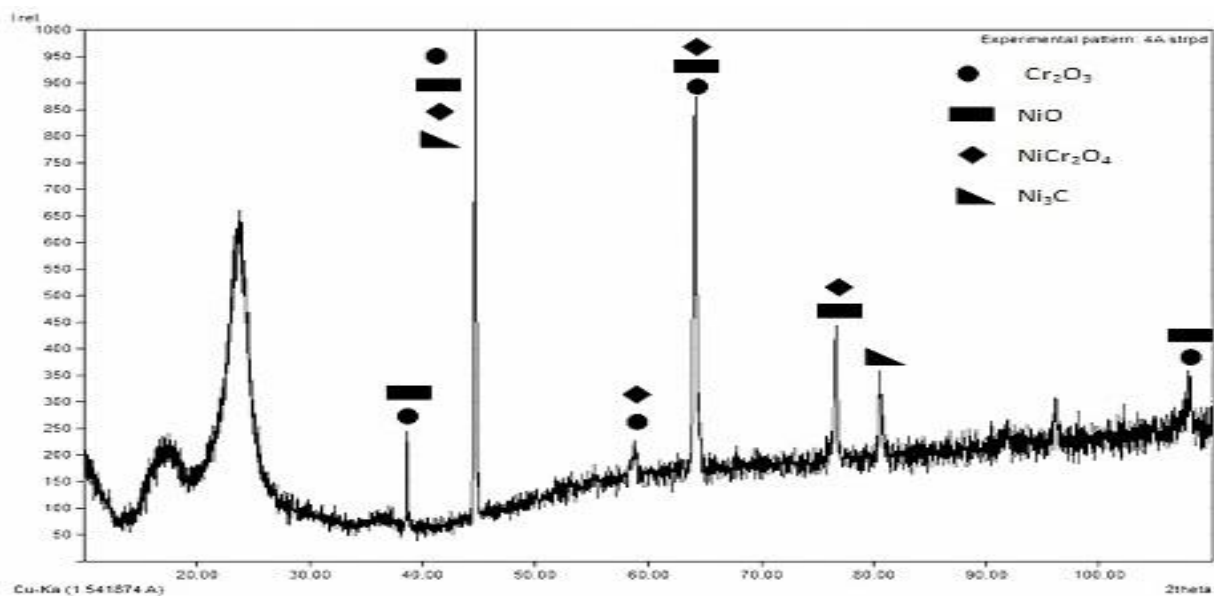


Figure.9

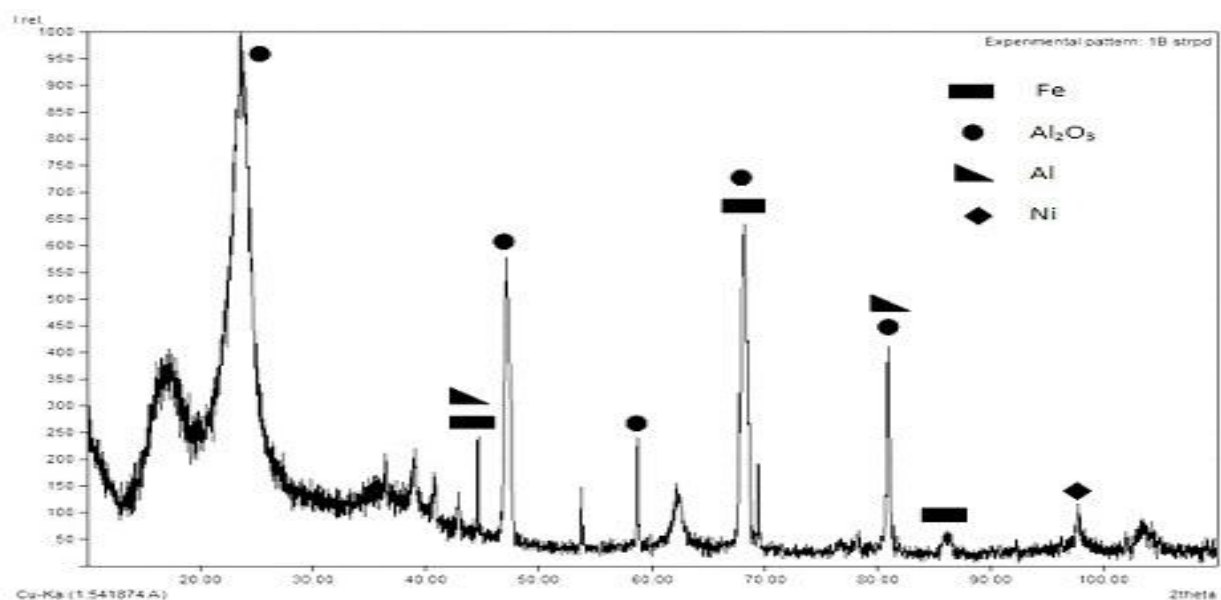


Figure.10

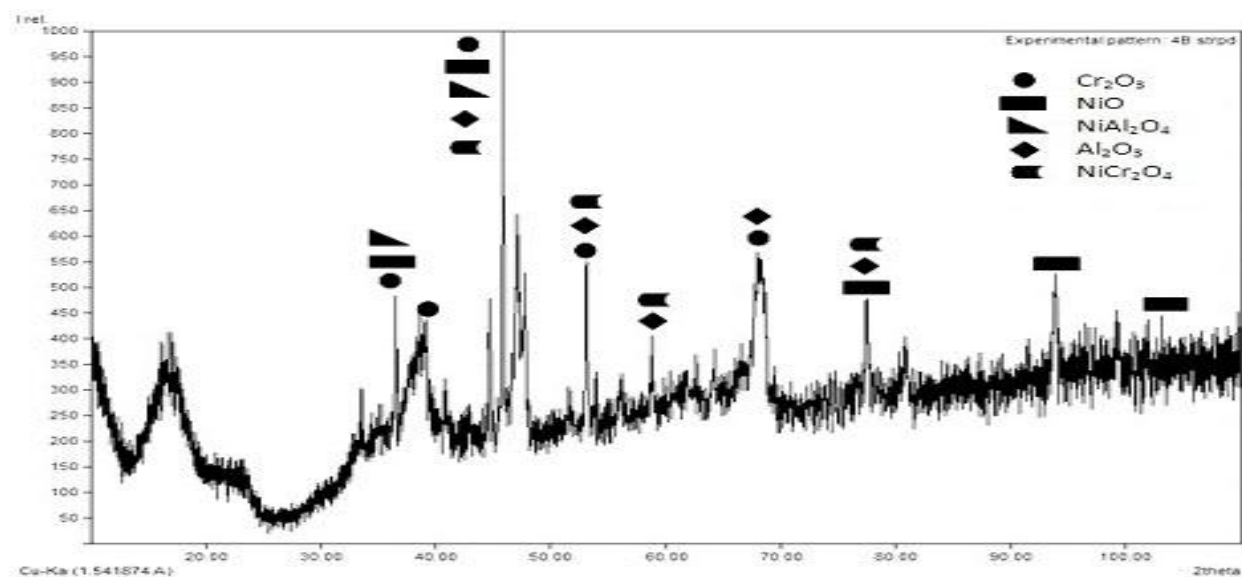


Figure.11

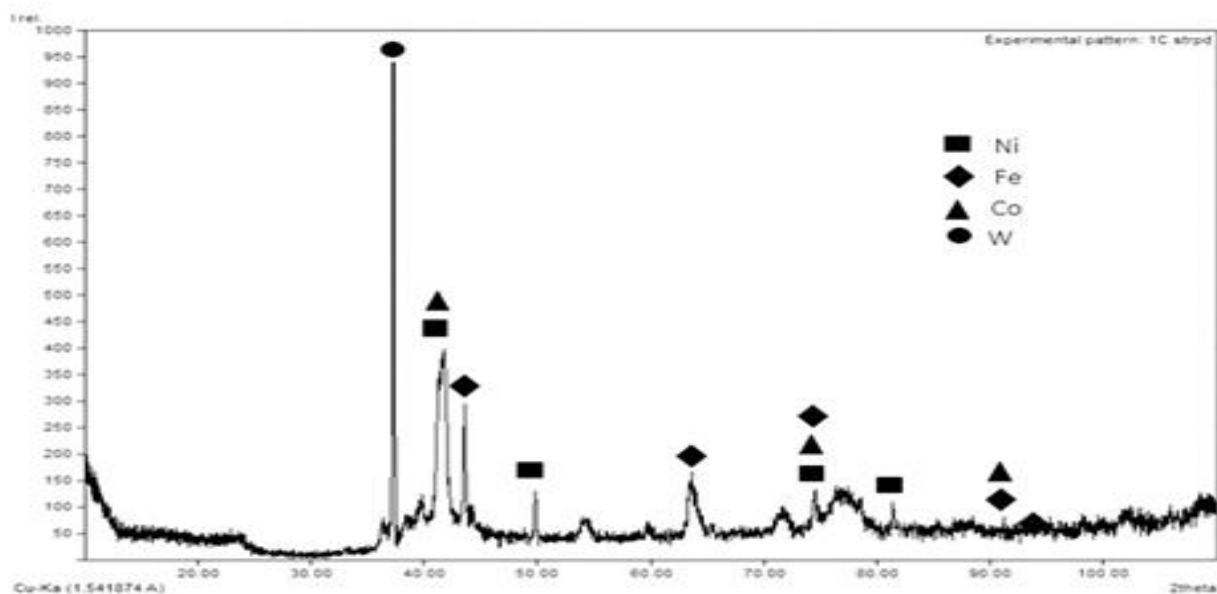


Figure.12

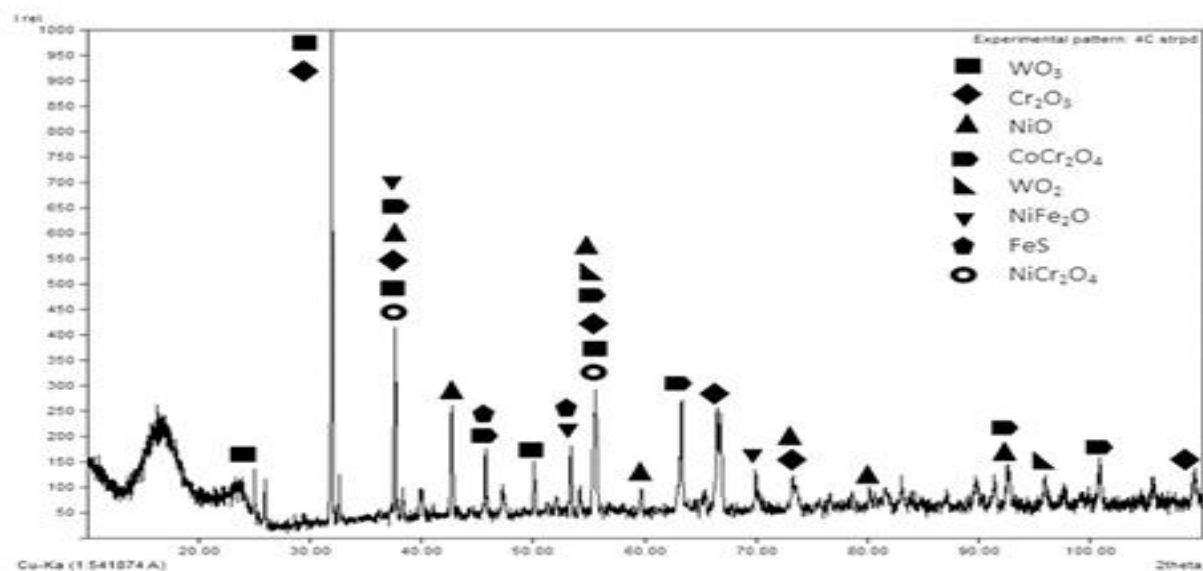


Figure.13

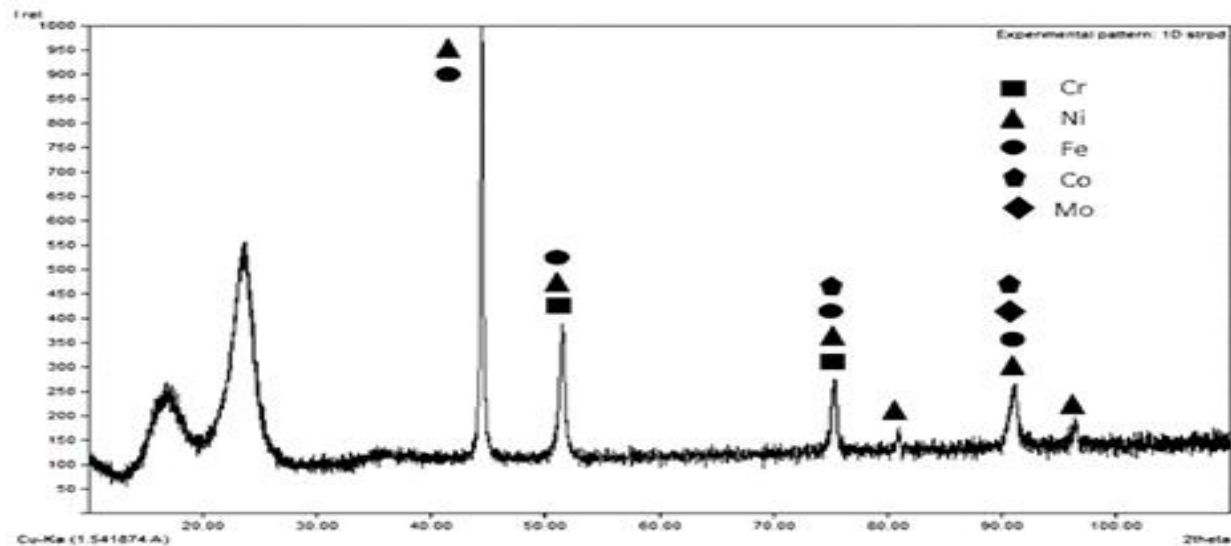


Figure.14

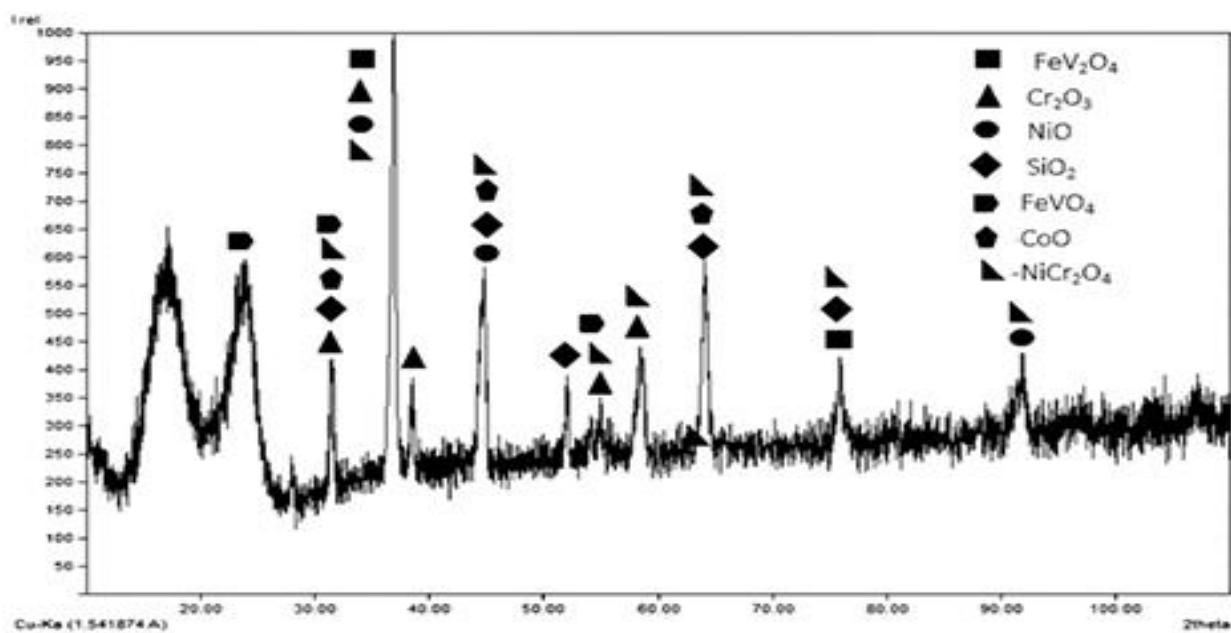


Figure.15

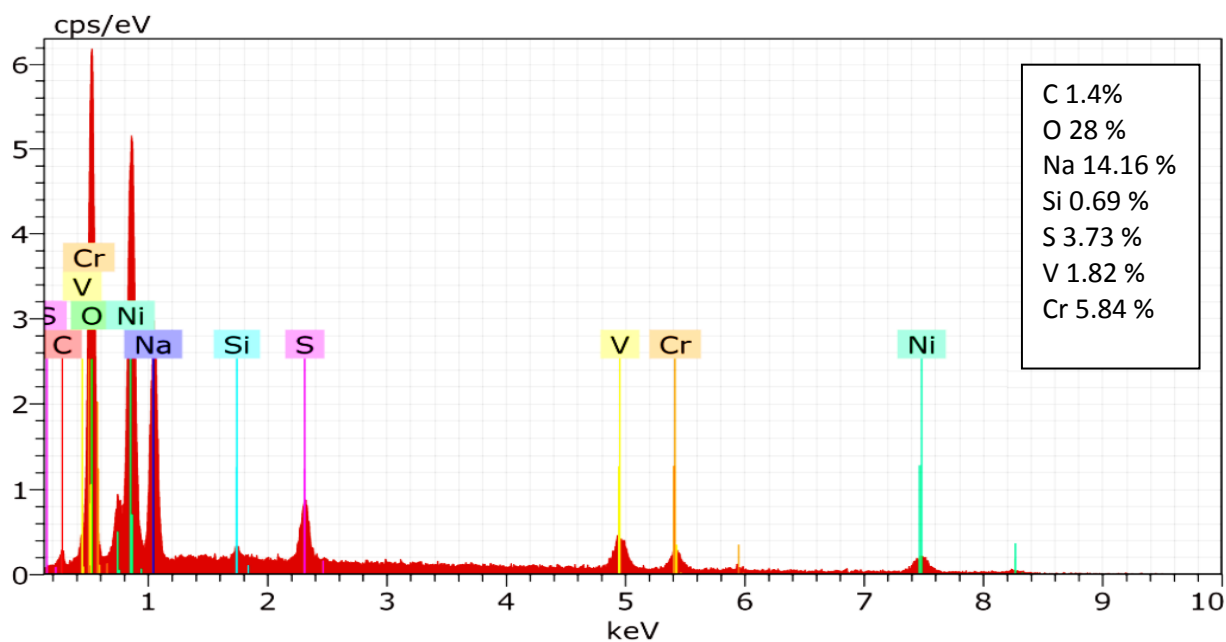
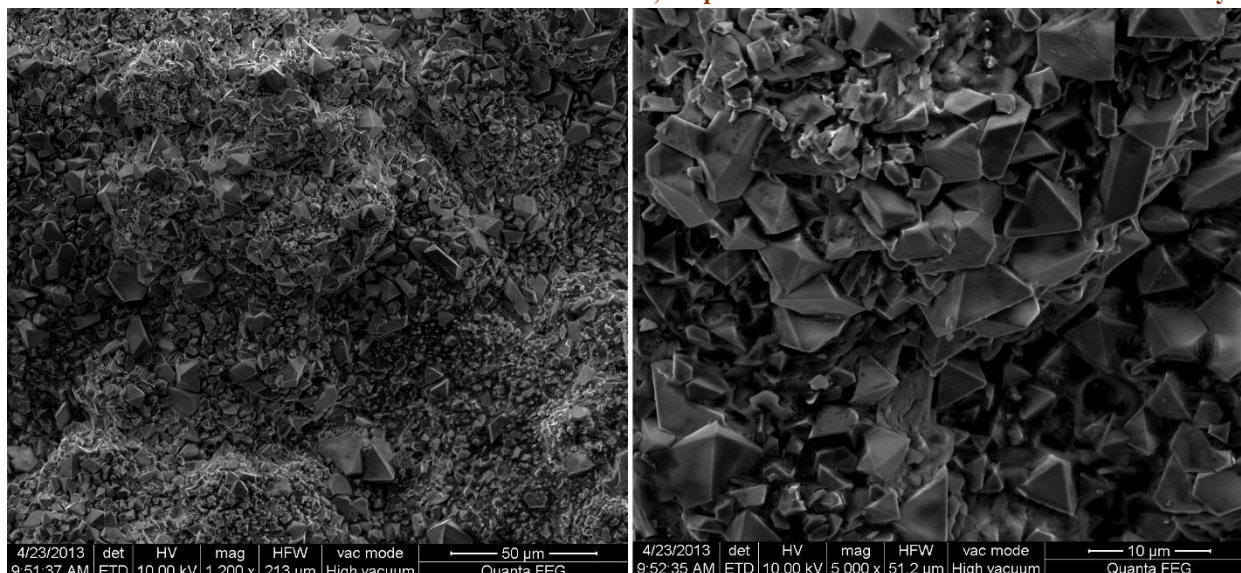


Figure.16

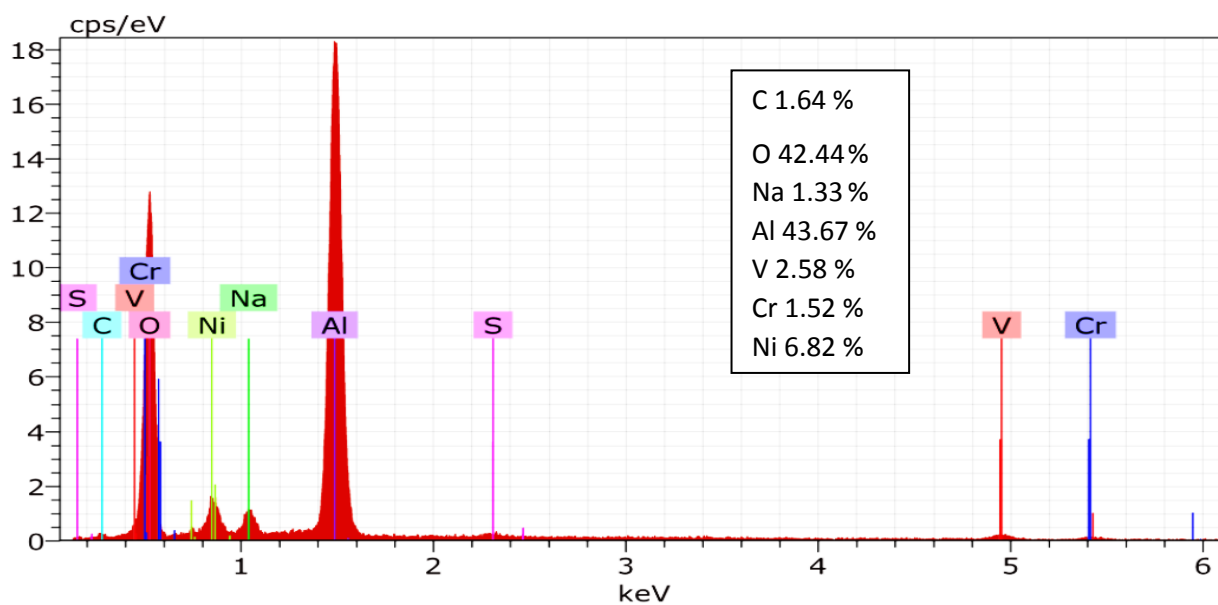
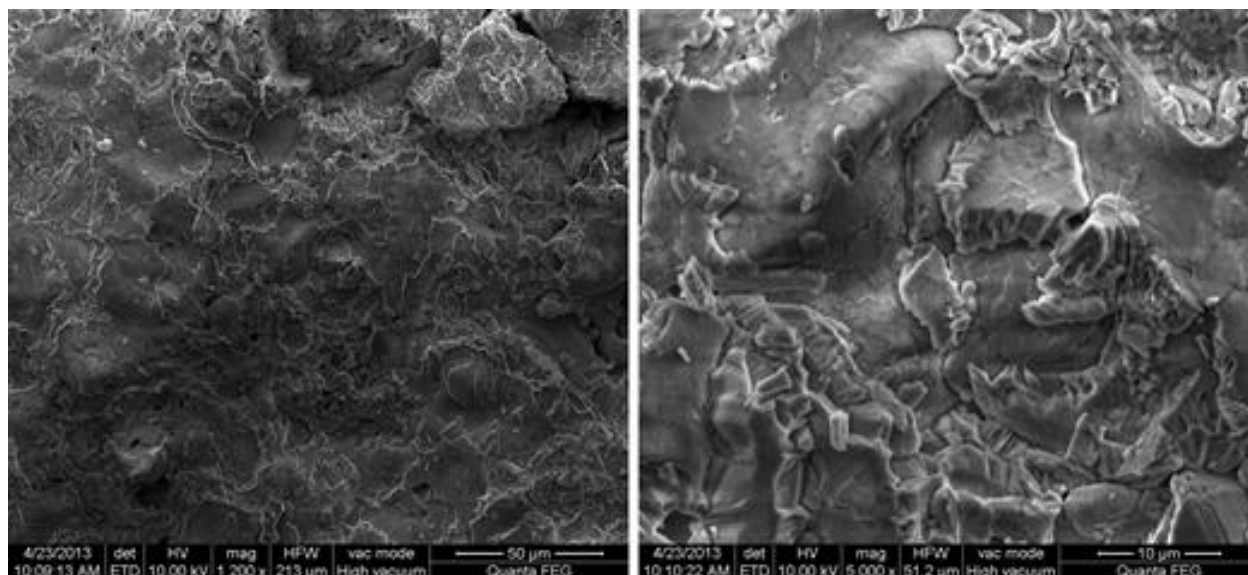


Figure.17

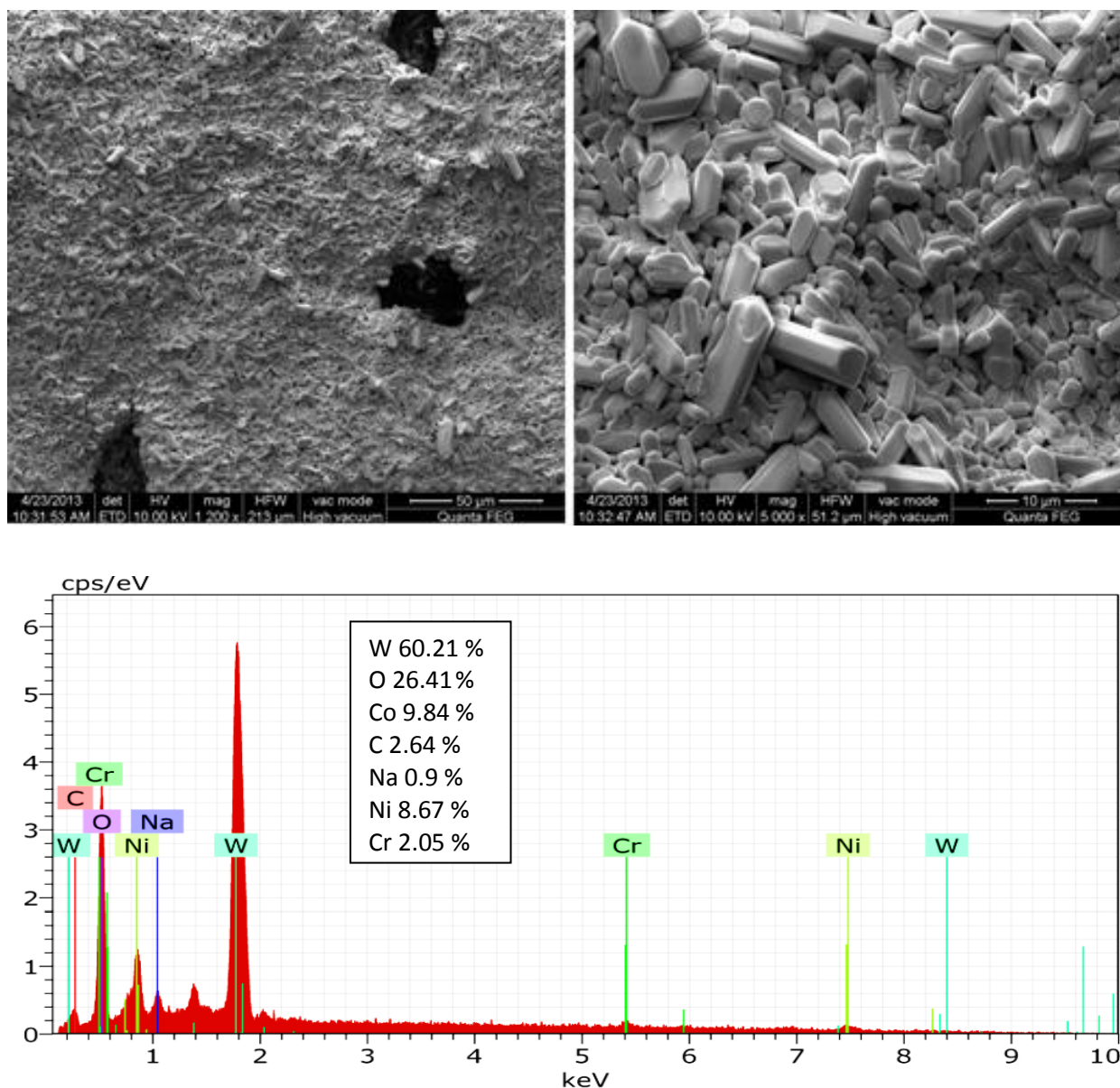


Figure.18

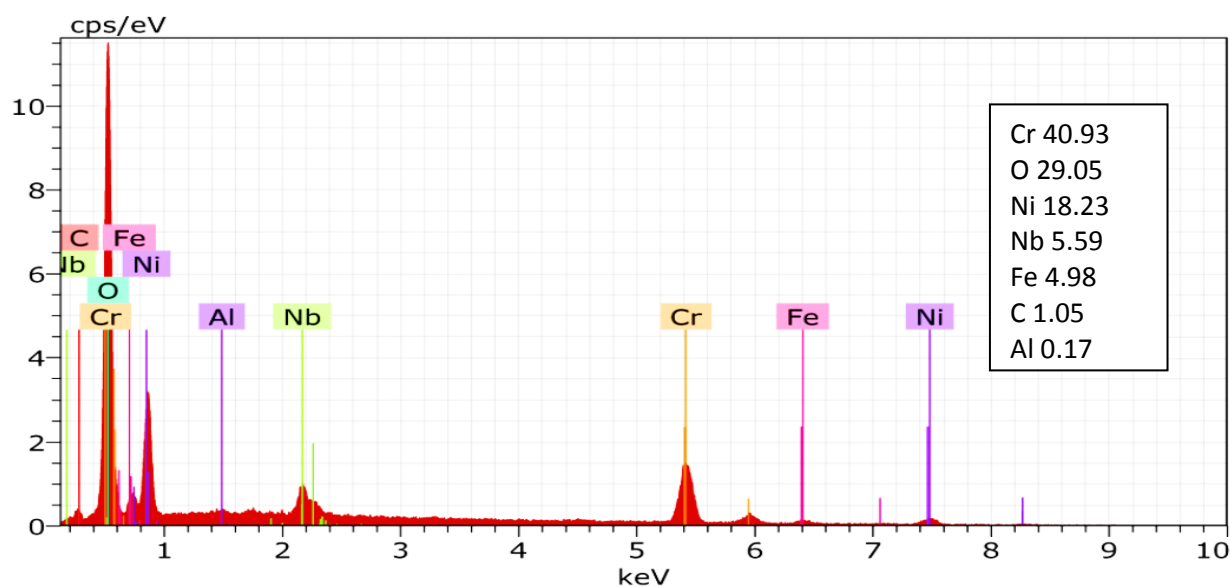
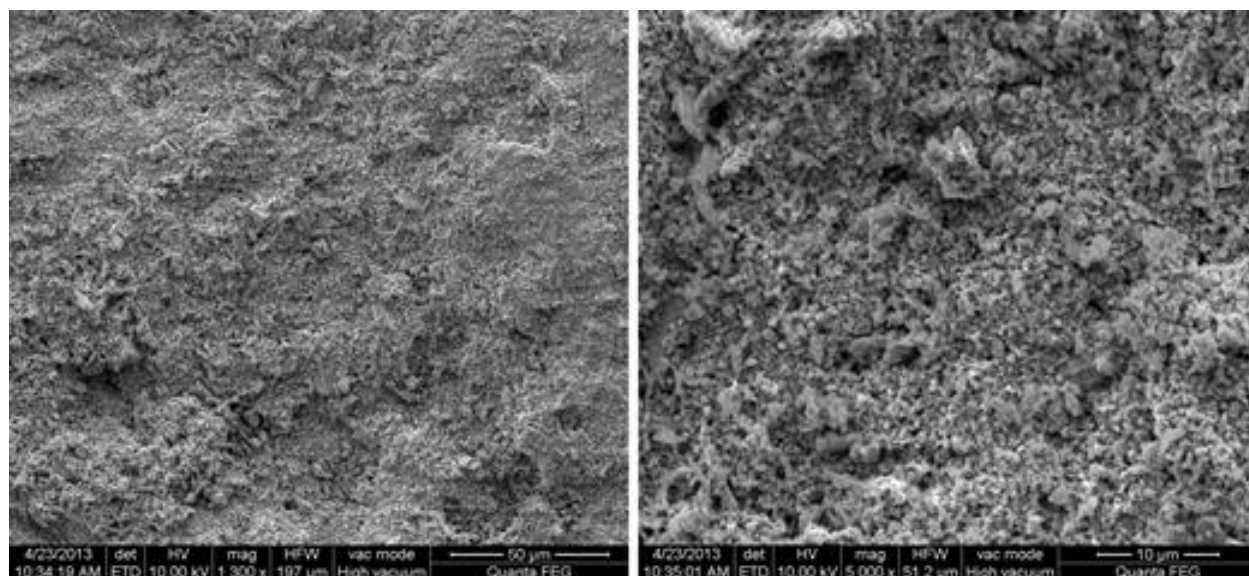


Figure.19

Legends for Figures

Figure . 1. Photograph of (a) un-coated; (b) WC; (c) Ni-Cr and (d) Al₂O₃coated Inconel-625 substrate.

Figure. 2. Photograph of hot corroded samples at 900°C after 50 cycles.

(a) Ni-Cr coated after molten salt corrosion; (b) Un-coated samples after molten salt corrosion(c) Ni-Cr coated air oxidation; (d) Un-coated air oxidation; (e) Ni-Cr coated after air oxidation(f) Al₂O₃ coated after Air Oxidation; (g) WC coated air oxidation; (h) Un-coated air oxidation.

Figure. 3. Comparison of Weight gain/area for the uncoated and Plasma spray coated Ni-Cr Inconel-625 samples subjected to hot corrosion in Molten Salt and Air Oxidation Modes.

Figure. 4. Comparison of Weight change/area vs. number of cycles plot for the uncoated and Plasma spray coated Ni-Cr Inconel-625 subjected to hot corrosion in Na₂SO₄-60% V₂O₅environment at 900°C for 25 cycles.

Figure. 5. Comparison ofWeight change/area vs. number of cycles plot for the uncoated and Plasma spray coated Ni-Cr Inconel-625 subjected to hot corrosion in airat 900°C for 25 cycles.

Figure. 6. (Weight change/area)² vs. number of cycles plot for Plasma spray coated Ni-Cr Inconel-625 subjected to hot corrosion at 900°C for 25 cycles.

Figure. 7. (Weight change/area)² vs. number of cycles plot for uncoatedInconel-625 subjected to hot corrosion at 900°C for 25 cycles.

Figure. 8. XRD Pattern of Ni-Cr coated Inconel-625 prior to hot corrosion.

Figure. 9. XRD Pattern of Ni-Cr coated Inconel-625 after hot corrosion in Molten Salt Environment.

Figure. 10. XRD Pattern of Al₂O₃coated Inconel-625 prior to hot corrosion

Figure. 11. XRD Pattern of Al₂O₃ coated Inconel-625 after hot corrosion in Molten Salt Environment.

Figure. 12. XRD Pattern of WC coated Inconel–625 prior to hot corrosion.

Figure. 13. XRD Pattern of WC coated Inconel–625 after hot corrosion in Molten Salt Environment.

Figure. 14. XRD Pattern of uncoated Inconel–625 specimen prior to hot corrosion.

Figure. 15. XRD Pattern of uncoated Inconel–625 after hot corrosion in Molten Salt Environment.

Figure. 16. SEM/EDAX of Ni–Cr coated Inconel–625 after corrosion in molten salt.

Figure. 17. SEM / EDAX of Al₂O₃ coated Inconel–625 after corrosion in molten salt.

Figure. 18. SEM/EDAX of WC coated Inconel–625 after corrosion in molten salt.

Figure. 19. SEM/EDAX of uncoated Inconel–625 after corrosion in molten Salt.